Voxel-based quantitative susceptibility mapping revealed increased cerebral iron over the whole brain in chronic migraine

Zhiye Chen[1,2], Wei Dai[3] $\circledcirc$, Xiaoyan Chen[3], Mengqi Liu[1,4], Lin Ma[4], and Shengyuan Yu[3] $\circledcirc$

Abstract

Background: The previous documents demonstrated that iron deposition was identified in brain deep nuclei and peri-aqueductal gray matter region in chronic migraine (CM), and less is known about the cerebral iron deposition in CM. The aim of this study is to investigate the cerebral iron deposition in CM using an advanced voxel-based quantitative susceptibility mapping.

Methods: A multi-echo gradient echo MR sequence was obtained from 14 CM patients and 28 normal controls (NC), and quantitative susceptibility mapping images were reconstructed and voxel-based analysis was performed over the whole cerebrum. The susceptibility value of all the positive brain regions was extracted and correlation was calculated between the susceptibility value and the clinical variables.

Results: The brain regions with increased susceptibility value in CM patients located in right precuneus, insula, supra-marginal gyrus, dorsolateral superior frontal gyrus, postcentral gyrus, cuneus and left postcentral gyrus compared with NC. The correlation analysis demonstrated that a positive correlation was identified between susceptibility value of all the positive brain regions and VAS score.

Conclusion: The current study demonstrated increased cerebral iron deposition presented in chronic patients, which suggested that increased cerebral iron deposition might play a role in the migraine chronicization.

Keywords

Chronic migraine, iron deposition, quantitative susceptibility mapping, magnetic resonance imaging, brain

Introduction

Chronic migraine (CM) is defined as at least 15 days of headache per month for more than 3 months, including at least eight days a month on which the headache feature and associated symptoms are fully developed migraine attacks.[1] It is estimated that CM affects 1.4–2.2% of the general population globally[2] and around 3% of episodic migraine (EM) patients evolve to CM each year.[3] The etiopathogenesis of migraine are hypothesized to be various processes and mechanisms involving activation of the trigeminal nerve system, abnormality of brain structure and function, vasoconstriction and vasodilation, and cortical spreading depression,[4] among which the cerebral cortices serve a vital role. Structural and functional alterations of cerebral

[1]Department of Radiology, Hainan Hospital of Chinese PLA General Hospital, Sanya, China
[2]The Second School of Clinical Medicine, Southern Medical University, Guangzhou, China
[3]Department of Neurology, First Medical Center of Chinese PLA General Hospital, Beijing, China
[4]Department of Radiology, First Medical Center of Chinese PLA General Hospital, Beijing, China

The first two authors contributed equally to this work.

Corresponding Authors:
Lin Ma, Department of Radiology, First Medical Center of Chinese PLA General Hospital, 28 Fuxing Road, Beijing 100853, China.
Email: cjr.malin@vip.163.com
Shengyuan Yu, Department of Neurology, First Medical Center of Chinese PLA General Hospital, 28 Fuxing Road, Beijing 100853, China.
Email: yusy1963@126.com

cortices have been widely reported in migraine patients.[5] Cortical hyperexcitability and aberrant resting-state brain activity may underlie the cascade of migraine attacks.[6] Interfering with cortical activity can affect pain perception, while pain-related cortical regions undergoing changes in synaptic plasticity can generate pain perception even with no detectable sensory input from the periphery.[7]

Increased iron deposition in the brain has been described in migraine patients. Different MRI techniques have been used to measure brain iron concentrations in migraine, including susceptibility weighted imaging (SWI), T2 gradient echo imaging, T2 turbo spin echo sequence, transverse relaxation rates R2, and quantitative T2*.[8–12] Quantitative susceptibility mapping (QSM) is a noninvasive MRI technique that measures spatial distribution of magnetic susceptibility using phase images of gradient-recalled echoes.[13] It is validated that susceptibility measured by QSM is linearly correlated with concentration of iron in brain nuclei[14] and thus provides us an effective way to detect iron deposition in the brain.

Among the studies probing into the iron deposition in migraine brain, increased iron deposition level has been described in periaqueductal gray matter (PAG), red nucleus, globus pallidus and putamen in migraine patients compared to controls using MRI.[9–12] While most of these researches focus iron deposition on the deep brain nuclei and PAG regions, cerebrum has been randomly studied. In our study we aim to investigate cerebral iron deposition in CM by voxel-based QSM technique.

Materials and methods

Subjects

The written informed consents were obtained from all subjects according to the approval of the ethics committee of local institutional review board. Fourteen chronic migraine patients [4 males and 10 females, mean age 41.71 ± 8.87 years] and 28 normal controls [10 males and 18 females, mean age 42.36 ± 11.10 years] were sequentially recruited from Headache Clinic and the staffs of Chinese PLA General Hospital.

All the patients should meet the International Classification of Headache Disorders, 3rd Edition (ICHD-III) criteria of chronic migraine without aura.[1] The inclusion criteria should fulfil the following conditions: (1) the diagnosis of migraine and CM refers to 1.1 Migraine without aura and 1.3CM in ICHD-III, respectively; (2) without migraine preventive medication in the past 3 months; (3) absence of other subtypes of headache, chronic pain other than headache, severe anxiety or depression, and psychiatric diseases; (4) absence of alcohol, nicotine, or other substance abuse. The exclusion criteria should meet the following conditions: cranium trauma, the cerebrovascular disease, long-standing hypertension, diabetes mellitus, tumor history and brain surgery. All the subjects should have no MRI contraindications such as metal clips within the body and claustrophobia.

All the patients were performed with the Visual Analog Scale (VAS), Migraine Disability Assessment Scale (MIDAS), Hamilton Anxiety Scale (HAMA), Hamilton Depression Scale (HAMD) and Montreal Cognitive Assessment (MoCA) evaluation.

MR data acquisition

All MRI data was acquired using a conventional eight channel phased-array head coil on a GE three-tesla MR scanner (DISCOVERY MR750, GE Healthcare, Milwaukee, WI, USA). A multi-echo gradient echo sequence was used to reconstruct QSM images with the following parameters: first echo time (TE) = 4.72 ms, the last TE = 22.96 ms, deltaTE = 3.648 ms, repetition time (TR) = 26.7 ms, flip angle (FA) = 15°, field of view (FOV) = 22 × 22 cm and matrix = 416 × 320, slice thickness = 1.2 mm, slice gap = -0.6 mm, number of averages = 1. The brain structural images were obtained from a 3 D T1 gradient echo sequence with the following parameters: TE = 3.0 ms, TR = 7.0 ms, inversion time = 400 ms, FA = 12°, FOV = 25.6 × 25.6 cm and matrix = 256 × 256, slice thickness = 1.0 mm, slice gap = -0.6 mm, number of averages = 1. All the MR imaging protocols were identical for two 3.0 T MR scanner.

Imaging analysis

Imaging analysis was performed under MATLAB R2013b (version 8.2.0.701) (The Mathworks, Natick, MA, USA) environment. The QSM images were reconstructed by STI Suite (V3.0) software (STI.SUITE. MRI@gmail.com). The imaging coregister, normalization and voxel-based analysis were performed with Statistical Parameters Mapping (SPM) (v12.0) software (https://www.fil.ion.ucl.ac.uk/spm/software/).

The image processing steps included as following: (1) The magnitude images and phase images were imported into the STI software and then automatically generated magnetic susceptibility images; (2) 3 D T1 images (Figure 1(a)) were coregistered with the magnitude images (TE = 4.72 ms) (Figure 1(b)), and then generated the warped T1 images (Figure 1(c)); (3) The warped T1 images were normalized with the T1 template (provided by the SPM software) (Figure 1(d)), and then generated
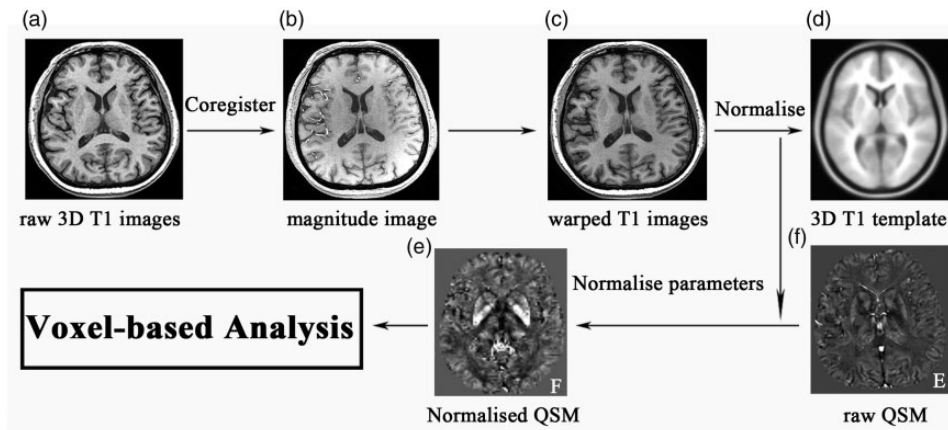
Figure 1. The flow chart of voxel-based quantitative susceptibility mapping: (1) 3 D T1 images (a) were coregistered with the magnitude images (TE = 4.72 ms) (b), and then generated the warped T1 images (c); (2) The warped T1 images (c) were normalized with the T1 template (d), and then generated the normalized parameters; (3) The normalized parameters were applied with the raw quantitative susceptibility images (e), and then generated the normalized susceptibility images (f), and then all the normalized images were smoothed by 8 mm full width at half maximum (FWHM) for further voxel-based analysis.

the normalized parameters; (4) The normalized parameters were applied with the raw quantitative susceptibility images (Figure 1(e)), and then generated the normalized susceptibility images (Figure 1(f)), and then all the normalized images were smoothed by 8 mm full width at half maximum(FWHM); (5) voxel-based analysis was performed using two-sample t-test between CM and NC. Significance difference was set at a P value of < 0.001 without false discovery rate (FDR) correction; (6) all the positive clusters were saved as a binary regions of interest (ROI) to extract the susceptibility value.

Statistical analysis

The data with normal distribution was described as mean±standard deviation. Correlation analysis was performed between susceptibility value of all the positive brain regions and the clinical variables, P value of <0.05 was considered to indicate a statistically significant correlation.

Results

Voxel-based QSM over the whole cerebrum in chronic migraine patients

Figure 2 presented that the brain regions with increased susceptibility value located in right supramarginal gyrus, precuneus, dorsolateral superior frontal gyrus, postcentral gyrus, cuneus, insula and left postcentral gyrus (Table 1). There were no brain regions with decreased susceptibility value over the whole cerebrum.

Correlation analysis between the susceptibility value of all the positive brain regions and the clinical variables

Table 2 presented that there was a significant positive correlation between the susceptibility value of all the brain regions with increased iron (0.010 ± 0.004) and VAS score (r = 0.0555, P value = 0.039). The other clinical variables, including MIDAS, diseased duration, headache frequency, HAMA, HAMD and MoCA socre, showed no significant correlation with the susceptibility value (P value > 0.05).

Discussion

Although iron deposition in the migraine brain has been studied in the past 20 years,[9,12] which mainly revealed the increased iron deposition in PAG in EM and chronic daily headache patients, and higher iron level in putamen, globus pallidus and red nucleus in migraineurs under age of 50, the altered cerebral iron deposition over the whole gray matter was not reported in CM patients up to now.

The current study demonstrated that the elevated iron deposition was identified in several cortical regions in CM patients by an advanced voxel-based QSM technique, which indicated that the impaired iron homeostasis in CM was not limited to the deep brain nuclei and PAG,[9,15] and the cortical regions with high iron deposition level might be another key center in generation and regulation of migraine.

The elevated iron deposition areas in this study located in right precuneus, insula, supramarginal gyrus, dorsolateral superior frontal gyrus, postcentral gyrus, cuneus and left postcentral gyrus. Iron can generate
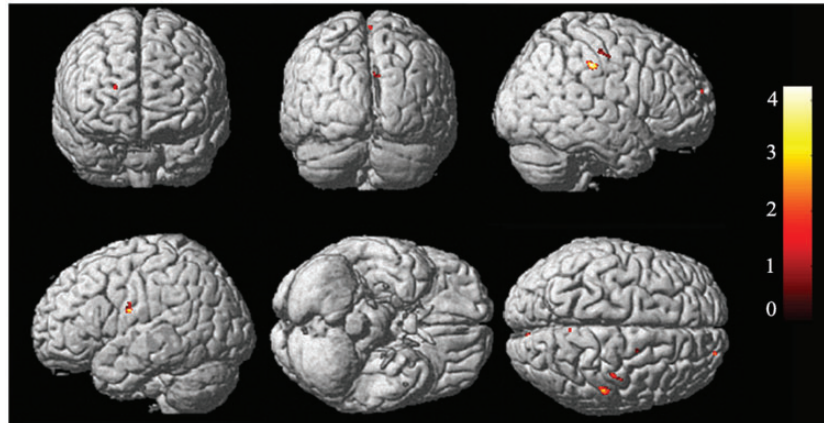
Figure 2. The brain regions with increased susceptibility value over the whole cerebrum in chronic migraine patients, which located in the right supramarginal gyrus, precuneus, dorsolateral superior frontal gyrus, postcentral gyrus, cuneus, insula and left postcentral gyrus.

Table 1. The brain regions with increased susceptibility value over the whole cerebrum in chronic migraine patients.

Anatomic region	MNI-space			Cluster size	T value
	X	Y	Z		
Right supramarginal gyrus	50	−26	39	250	4.268
Left postcentral gyrus	−53	−6	22	105	4.260
Right precuneus	3	−54	69	22	3.897
Right dorsolateral superior frontal gyrus	21	62	19	28	3.792
Right postcentral gyrus	40	−19	50	61	3.778
Right dorsolateral superior frontal gyrus	19	0	54	22	3.770
Right insula	39	−20	12	22	3.687
Right cuneus	9	−78	30	14	3.678
Right cuneus	6	−87	32	13	3.633

Table 2. Correlation analysis between the susceptibility value of all the positive brain regions and clinical variables.

Variables	Mean±SD	r	P value	95%CI for r
VAS	7.930 ± 1.439	0.555	0.039	0.035 to 0.086
MIDAS	101.357 ± 56.291	0.226	0.438	−0.347 to 0.675
DD (years)	11.714 ± 9.507	0.183	0.532	−0.385 to 0.650
HF[†]	25.929 ± 5.717	−0.456	0.102	−0.794 to 0.099
HAMA	23.429 ± 10.353	−0.353	0.215	−0.744 to 0.218
HAMD	17.714 ± 10.484	−0.082	0.781	−0.587 to 0.469
MoCA	23.357 ± 4.684	−0.472	0.088	−0.802 to 0.078

[†]The number of headache attack per month.
VAS, Visual Analog Scale; MIDAS, Migraine Disability Assessment Scale; DD, disease duration; HF, headache frequency; HAMA, Hamilton Anxiety Scale; HAMD, Hamilton Depression Scale; MoCA, Montreal Cognitive Assessment; r, correlation coefficient; CI, confidence interval.

reactive oxygen species, and both iron and reactive oxygen species are indicated to be important initiators and mediators of cell death.[16] The increased iron deposition in precuneus and insula might explain the decreased the resting functional connectivity density of precuneus[17] and decreased gray matter volume of insula[18] in CM, which would also provide valuable information to understand the neuromechanism of the cognitive modulation of pain sensitivity,[19] pain experience and expectation,[20,21] and pain catastrophizing on mild pain[22] in CM.

The postcentral gyrus is responsible for recognizing the localization and intensity of pain[23] and the supramarginal gyrus interprets tactile sensory information.[24]

The elevated iron deposition of bilateral postcentral gyrus and right supramarginal gyrus might influence the pain matrix network, including the anterior insula, precuneus, supramarginal gyrus, thalami and several other regions, which would increase the functional connectivity of the pain matrix and might play a role in migraine chronicization in CM.[25] The dorsolateral prefrontal cortex (DLPFC) is a large and substantially heterogeneous brain region, which was considered as a key node of networks implicated in nociceptive processing and pain modulation.[26] This study demonstrated that high iron deposition of DLPFC might depict the possible pathophysiological basis for the decreased functional connectivity to nodes of the default mode network (DMN) in CM.[27]

The iron deposition in the cerebral cortex also added more support of cortical dysfunction in the pathogenesis mechanism of migraine chronicization. Moreover, higher VAS scores were associated with increased iron deposition in cerebral cortex in migraine patients in the current study, which suggested that the iron accumulation level in CM was related to the severity of headache attacks. It remained unclear whether iron accumulation in the cortex had a causative role in the development of chronic migraine headache or the consequence of repetitive of migraine attack.

The QSM technique was firstly used to evaluate the cerebral iron deposition in CM patients. QSM may provide an effective as well as noninvasive way of revealing iron deposition in the brain in vivo. Previous studies[28,29] usually used phase imaging or susceptibility weighted imaging (SWI) for iron evaluation, which may yield to nonlocal field influence that caused by calcifications and vessels and result lower sensitivity to local susceptibility effects caused by iron on 1.5 T MR scanner. Meanwhile, the voxel-based analysis of QSM was also performed over the whole brain in this study, which presented relative objective and reliable.

This study has some limitations as following: (1) The sample size of CM was relatively small although the voxel-based analysis was used; (2) The other MRI patterns was not used in the current study, such as gray matter volume, resting-state functional connectivity and perfusion imaging; (3) We are not able to draw the causative relationship of the iron deposition in cortex and migraine chronicization.

In conclusion, the increased iron deposition was observed in cerebral cortical regions in CM, and positively related with pain intensity, which indicated that increased cerebral iron deposition might play a role in the migraine chronicization. The voxel-based QSM could be considered as a simple and effective tool to evaluate the brain iron accumulation in migraine neuroimaging.

ORCID iDs

Wei Dai https://orcid.org/0000-0002-7015-2531
Shengyuan Yu https://orcid.org/0000-0001-8933-088X

References

1. Headache Classification Committee of the International Headache Society. The international classification of headache disorders, 3rd edition. *Cephalalgia* 2018; 38: 1–211.
2. Natoli JL, Manack A, Dean B, Butler Q, Turkel CC, Stovner L, Lipton RB. Global prevalence of chronic migraine: a systematic review. *Cephalalgia* 2010; 30: 599–609.
3. Lipton RB, Fanning KM, Serrano D, Reed ML, Cady R, Buse DC. Ineffective acute treatment of episodic migraine is associated with new-onset chronic migraine. *Neurology* 2015; 84: 688–695.
4. Charles A. The pathophysiology of migraine: implications for clinical management. *Lancet Neurol* 2018; 17: 174–182.
5. Jia Z, Yu S. Grey matter alterations in migraine: a systematic review and meta-analysis. *Neuroimage Clin* 2017; 14: 130–140.
6. Liu H, Ge H, Xiang J, Miao A, Tang L, Wu T, Chen Q, Yang L, Wang X. Resting state brain activity in patients with migraine: a magnetoencephalography study. *J Headache Pain* 2015; 16: 525.
7. Zhuo M. A synaptic model for pain: long-term potentiation in the anterior cingulate cortex. *Mol Cells* 2007; 23: 259–271.
8. Palm-Meinders IH, Koppen H, Terwindt GM, Launer LJ, van Buchem MA, Ferrari MD, Kruit MC. Iron in deep brain nuclei in migraine? CAMERA follow-up MRI findings. *Cephalalgia* 2017; 37: 795–800.
9. Kruit MC, Launer LJ, Overbosch J, van Buchem MA, Ferrari MD. Iron accumulation in deep brain nuclei in

migraine: a population-based magnetic resonance imaging study. *Cephalalgia* 2009; 29: 351–359.

10. Tepper SJ, Lowe MJ, Beall E, Phillips MD, Liu K, Stillman MJ, Horvat M, Jones SE. Iron deposition in pain-regulatory nuclei in episodic migraine and chronic daily headache by MRI. *Headache* 2012; 52: 236–243.

11. Dominguez C, Lopez A, Ramos-Cabrer P, Vieites-Prado A, Perez-Mato M, Villalba C, Sobrino T, Rodriguez-Osorio X, Campos F, Castillo J, Leira R. Iron deposition in periaqueductal gray matter as a potential biomarker for chronic migraine. *Neurology* 2019; 92: e1076–e1085.

12. Welch KM, Nagesh V, Aurora SK, Gelman N. Periaqueductal gray matter dysfunction in migraine: cause or the burden of illness? *Headache* 2001; 41: 629–637.

13. Liu C, Wei H, Gong NJ, Cronin M, Dibb R, Decker K. Quantitative susceptibility mapping: contrast mechanisms and clinical applications. *Tomography* 2015; 1: 3–17.

14. Langkammer C, Schweser F, Krebs N, Deistung A, Goessler W, Scheurer E, Sommer K, Reishofer G, Yen K, Fazekas F, Ropele S, Reichenbach JR. Quantitative susceptibility mapping (QSM) as a means to measure brain iron? A post mortem validation study. *Neuroimage* 2012; 62: 1593–1599.

15. Kruit MC, van Buchem MA, Launer LJ, Terwindt GM, Ferrari MD. Migraine is associated with an increased risk of deep white matter lesions, subclinical posterior circulation infarcts and brain iron accumulation: the population-based MRI CAMERA study. *Cephalalgia* 2010; 30: 129–136.

16. Dixon SJ, Stockwell BR. The role of iron and reactive oxygen species in cell death. *Nat Chem Biol* 2014; 10: 9–17.

17. Dai L, Yu Y, Zhao H, Zhang X, Su Y, Wang X, Hu S, Dai H, Hu C, Ke J. Altered local and distant functional connectivity density in chronic migraine: a resting-state functional MRI study. *Neuroradiology* 2021; 63: 555–562.

18. Chen WT, Chou KH, Lee PL, Hsiao FJ, Niddam DM, Lai KL, Fuh JL, Lin CP, Wang SJ. Comparison of gray matter volume between migraine and "strict-criteria" tension-type headache. *J Headache Pain* 2018; 19: 4.

19. Goffaux P, Girard-Tremblay L, Marchand S, Daigle K, Whittingstall K. Individual differences in pain sensitivity vary as a function of precuneus reactivity. *Brain Topogr* 2014; 27: 366–374.

20. Bantick SJ, Wise RG, Ploghaus A, Clare S, Smith SM, Tracey I. Imaging how attention modulates pain in humans using functional MRI. *Brain* 2002; 125: 310–319.

21. Koyama T, McHaffie JG, Laurienti PJ, Coghill RC. The subjective experience of pain: where expectations become reality. *Proc Natl Acad Sci U S A* 2005; 102: 12950–12955.

22. Seminowicz DA, Davis KD. Cortical responses to pain in healthy individuals depends on pain catastrophizing. *Pain* 2006; 120: 297–306.

23. Almeida TF, Roizenblatt S, Tufik S. Afferent pain pathways: a neuroanatomical review. *Brain Res* 2004; 1000: 40–56.

24. Reed CL, Caselli RJ. The nature of tactile agnosia: a case study. *Neuropsychologia* 1994; 32: 527–539.

25. Lee MJ, Park BY, Cho S, Kim ST, Park H, Chung CS. Increased connectivity of pain matrix in chronic migraine: a resting-state functional MRI study. *J Headache Pain* 2019; 20: 29.

26. Seminowicz DA, Moayedi M. The dorsolateral prefrontal cortex in acute and chronic pain. *J Pain* 2017; 18: 1027–1035.

27. Hubbard CS, Khan SA, Keaser ML, Mathur VA, Goyal M, Seminowicz DA. Altered brain structure and function correlate with disease severity and pain catastrophizing in migraine patients. *eNeuro* 2014; 1: e2014.

28. Marques JP, Maddage R, Mlynarik V, Gruetter R. On the origin of the MR image phase contrast: an in vivo MR microscopy study of the rat brain at 14.1 T. *Neuroimage* 2009; 46: 345–352.

29. Rockwell DT, Melhem ER, Bhatia RG. GRASE (gradient- and spin-echo) MR of the brain. *AJNR Am J Neuroradiol* 1997; 18: 1923–1928.